The Histology of Skin Treated With a Picosecond Alexandrite Laser and a Fractional Lens Array

Emil A. Tanghetti, MD*
Center for Dermatology and Laser Surgery, 5601 J Street, Sacramento, California 95819

Background and Objectives: The treatment of acne scars and wrinkles with a picosecond Alexandrite laser was recently FDA cleared. In 2014 we presented our initial histologic findings with this device on *in vivo* and *ex vivo* skin. This current study expands on the 2014 pilot study with an investigation of different energy settings using histology and the confocal microscope to describe the changes observed in the skin.
Materials and Methods: We used a 755 nm picosecond Alexandrite laser with a fractional optic with three different energy settings to treat *in vivo*. After treatment, the patients and skin samples were also evaluated with a confocal microscope followed by biopsies which were evaluated histologically.
Results: Histology revealed unique intra-epidermal cavities. The number, density, and the size of these cavities were dependent on the melanin index and delivered energy when evaluated with histopathology and the confocal microscope. These localized zones of injury appear to form microscopic epidermal injury zones which are exfoliated over a 3-week period.
Conclusions: These intra-epidermal cavities result from areas of laser-induced optical breakdown (LIOB). This injury is most consistent with a localized plasma formation in the epidermis initiated by the melanin absorption of the high energy picosecond light. It appears that treatments with this device and optic result in improvements in dyspigmentation and acne scars with new collagen, elastic tissue, and mucin. The production of this LIOB could directly stimulate an epidermal repair mechanism that results in these clinical findings. Lasers Surg. Med.

Key words: diffractive lens array; laser induced optical breakdown; non-ablative

INTRODUCTION

The first picosecond laser for tattoo removal and pigment was a 755 nm Alexandrite laser cleared by the FDA in 2012. This device delivered a uniform beam profile over various spot sizes and fluences. A fractional treatment modality with a diffractive lens array optics [1–3] has been demonstrated on millisecond-pulsed laser systems for the treatment of acne scars and photo-damaged skin. These arrays created high fluence regions separated by a low fluence background to produce focal areas of ablative or non-ablative injury in the skin. To realize the advantages of a fractional treatment with the picosecond laser system, a hand piece with a diffractive lens array was added and this device received FDA clearance in 2014 for the treatment of acne scars and wrinkles.

Recently, Brauer et al. have reported their clinical findings using the fractional picosecond Alexandrite laser for the treatment of facial atrophic acne scars [4]. They noted improvement in the appearance of these abnormalities accompanied by an increase in dermal collagen, mucin, and density of elastic fibers. Subjects reported very low pain scores (2.8/10) with mild transient erythema and edema typically lasting 1–4 hours. Preliminary histologic findings *in vivo* for both the flat beam optic and lens array optic have revealed unique injury profiles [5,6]. In this report, the *in vivo* response to treatment with the lens array out to 14 days post-treatment is described and the injury profiles are further characterized with both histology and confocal microscopy. The results of this study will guide device parameter selection for skin rejuvenation, including treatment of pigmentary disorders, acne scars, and photo-damaged skin.

MATERIALS AND METHODS

A 755 nm picosecond Alexandrite laser with a diffractive lens array optic (Picosure^{TM}, Cynosure, Westford, MA) was used to treat *in vivo* skin at three different fluence and spot size settings (Table 1). The diffractive lens array consisted of closely packed individual hexagonal lenses with 500 μm pitch, the center-to-center lens distance. The diffractive lens array modifies the intensity profile of the Alexandrite laser beam to produce a hexagonal array of high intensity regions surrounded by low intensity background. Approximately 70% of the total energy is delivered in the high fluence regions comprising less than 10% of the treated

Conflict of Interest Disclosures: All authors have completed and submitted the ICMJE Form for Disclosure of Potential Conflicts of Interest and none were reported.
Contract grant sponsor: Cynosure, Inc.
*Correspondence to: Emil A. Tanghetti, MD, Center for Dermatology and Laser Surgery, 5601 J Street, Sacramento, CA 95819.
E-mail: et@dermatologyandlasersurgery.com
Accepted 9 May 2016
Published online in Wiley Online Library (wileyonlinelibrary.com).
DOI 10.1002/lsm.22540

TABLE 1. Average Fluence Versus Treatment Spot Size

Treatment spot diameter, mm	Average fluence, J/cm^2
6	0.71
8	0.40
10	0.25

area for a single non-overlapping pass. The remaining 30% of the energy provides the low fluence background (Fig. 1).

Men (3) and women (8) with Fitzpatrick Skin Types I–VI, ages 28–64 and melanin indices (MI) 10–35 including one subject with vitiligo, were treated on the back or volar forearm. Melanin index is proportional to the concentration of melanin in the skin with a range 0–99, where 0 is the whitest and 99 the darkest, and is measured with a pigment meter (Skintel^{TM}, Cynosure, Westford, MA). Fitzpatrick skin type (FST) is compared with melanin index in Figure 2. Treatment sites consisted of $2 \times 2\,cm^2$ squares within which one pass was performed for confocal imaging or three passes were delivered for biopsy to insure adequate sampling of the injury zones during serial, five micron sectioning. Biopsies with a 3.5 mm punch were taken and confocal imaging was performed both immediately and 24 hours after treatment. The biopsies were fixed in formalin and sections were stained with either hematoxylin and eosin (H&E) or Fontana Masson. Stained sections were examined with light microscopy by a pathologist and the investigator.

Microscopic analysis was performed on three-dimensional images taken immediately and 24 hours post treatment with a Vivascope 1500, Caliber Imaging and Diagnostics confocal microscope (formerly Lucid Inc., Andover, MA). Basic images are $50 \times 500\,\mu m^2$ tiles that are stitched together to provide a larger field of view, up to $8 \times 8\,mm^2$ at a given depth. Stitched images at different depths with 10 μm spacing were then stacked to form a three-dimensional cubic image for analysis. Photographs also were taken at the study visits. This investigation was approved by the New England Institutional Review Board and all subjects consented to participate in the study.

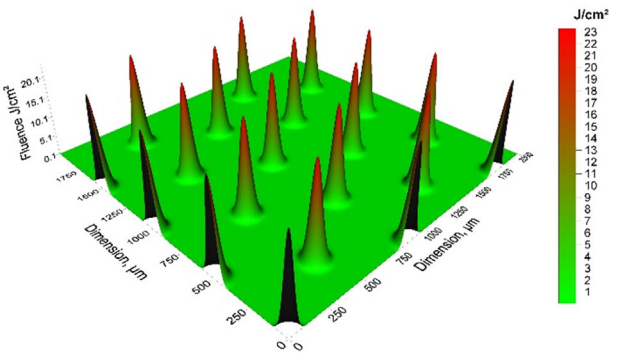

Fig. 1. Fluence distribution in the treatment plane on the skin surface. Treatment spot size 6 mm, peak fluences are 23 J/cm^2 and average fluence setting 0.71 J/cm^2.

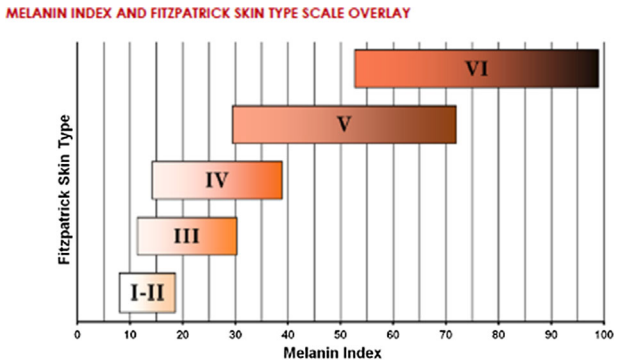

Fig. 2. Fitzpatrick Skin Type versus Melanin Index. A given melanin index value may correspond to multiple skin types because skin typing does not depend exclusively on melanin concentration.

RESULTS

Immediate post-treatment histology demonstrated well defined, approximately spherical, intra-epidermal spaces (vacuoles) void of H&E staining and measuring from 35 to 65 μm in diameter (Fig. 3). Degenerating necrotic keratinocytes were seen around the vacuoles but did not extend beyond one or two cellular layers. Location of the vacuoles varied from stratum granulosum to the dermal/epidermal junction. The vacuoles in tissue samples taken 24 hours after the treatment in darker skin types contained cellular

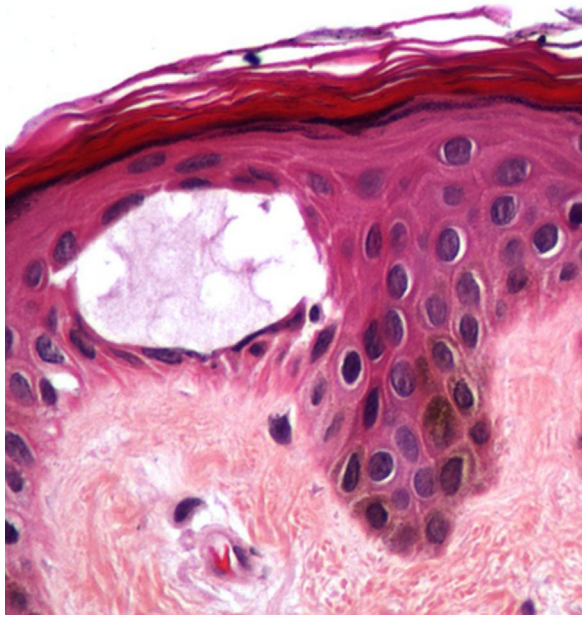

Fig. 3. Intra-epidermal vacuole in skin with FST III, MI = 23 measuring approximately 60 μm in diameter. Biopsy performed 10 minutes post treatment (600×).

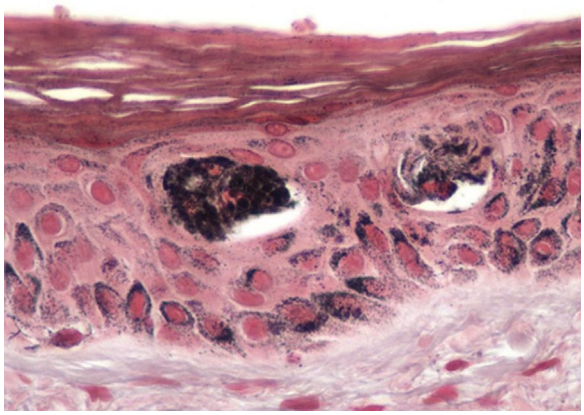

Fig. 4. Fontana Masson staining for melanin in skin type III, MI = 23 hours post treatment. Note the increased density of this staining in the vacuoles along with cellular debris. The underlying melanocytes, basal cells, and adjacent epidermal cells appear intact (600×).

debris positively stained with Fontana Masson, suggesting the presence of melanin (Fig. 4). Vacuoles found in lighter skin types MI ≤ 12 contained red blood cells. There was no apparent damage to surrounding cells or underlying structures found either immediately or 24 hours post treatment in any skin types.

The darker skin subjects presented clinically at 24 hours and up to 3 weeks post treatment with dark spots in a hexagonal pattern at a pitch matching that of the corresponding lens array for all fluences although the intensity of the darkened dots significantly decreased with lower fluences. As we decreased the energy, the vacuole diameter became smaller and the depth became deeper probably due to the increase in melanin density deeper in the epidermis as demonstrated in Figure 5 for a Hispanic subject with MI = 31. Mild to moderate lymphocytic perivascular inflammation was found in the papillary dermis [7]. In a lighter skinned subject with MI = 17, vacuoles were not seen with treatment fluence, $F = 0.25\,\mathrm{J/cm^2}$ but were seen at $F = 0.71\,\mathrm{J/cm^2}$ and $0.4\,\mathrm{J/cm^2}$ (Fig. 6). At 5 days and at 2 weeks post treatment zones of microscopic epidermal necrotic debris (MENDS) were seen immediately inferior to or within the stratum corneum (Fig. 7). These zones exfoliated around 3–5 weeks post treatment. Petechiae were observed in the lightest skinned subjects (MI < 12) increasing with higher fluence but with no discernable pattern. In contrast to the results in darker skin types, vacuoles were found only for the highest fluence, $F = 0.71\,\mathrm{J/cm^2}$ at or near the dermal/epidermal junction in subjects with low cutaneous melanin (MI = 10–12). These vacuoles were atypical, somewhat irregular in shape with less distinct borders, and were adjacent to dermal extravasation of red blood cells at the superficial capillary loops. At 24 hours post treatment, these vacuoles were seen filled with red blood cells (Fig. 8).

Confocal imaging immediately post treatment revealed no abnormalities in the epidermis or the papillary dermis for all subjects and treatment parameters. In light-skinned subjects with MI < 12 and the vitiligo subject, no signs of injury could be seen at any time point. However, 24 hours after treatment, well-defined spherical vacuoles characterized by bright areas in the image were observed but only for subjects with MI > 15 (Fig. 9). As the MI or fluence increased, the size and the density (number per unit area) of the vacuoles also increased. These vacuoles ranged in diameter from 25 to 70 μm and were located between 55 and 75 μm deep within the stratum spinosum. Figure 10 exhibits vacuole diameters versus treatment fluence in two darker-skinned subjects (MI = 31, 32). When adjacent confocal images of the darker skinned subjects were stitched to provide a larger surface area view, a hexagonal pattern of vacuoles emerged with a pitch approximately corresponding to that of the lens array optic used for the treatment (Fig. 11).

DISCUSSION

A 755 nm picosecond Alexandrite laser with a diffractive lens array optic delivered an array of unique, focal zones of

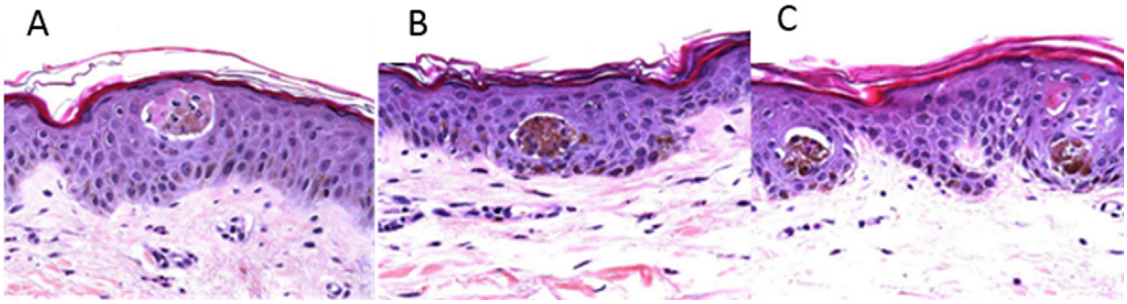

Fig. 5. Histology from a skin biopsy at 24 hours post treatment of skin type IV, MI = 31 demonstrating intra epidermal vacuoles created with $F =$ (**A**) $0.71\,\mathrm{J/cm^2}$, (**B**) $0.4\,\mathrm{J/cm^2}$, and (**C**) $0.25\,\mathrm{J/cm^2}$. The vacuoles contain cellular debris and the size and depth of the vacuole appears to diminish and increase, respectively, as the energy per micro-spot decreases. As we decrease the energy the vacuole diameter becomes smaller and the depth becomes deeper probably due to the increase in melanin density deeper in the epidermis (200×).

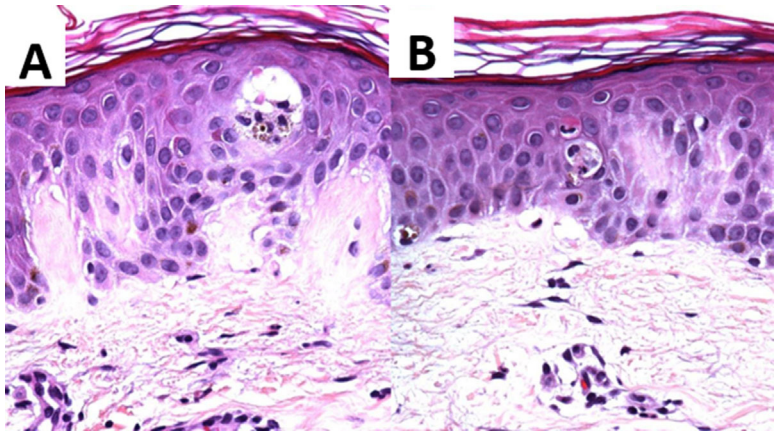

Fig. 6. Histology from a skin biopsy at 24 hours in an Asian patient skin type III MI = 17 on non sun-exposed skin demonstrating intra-epidermal vacuoles containing cellular debris with treatment fluence 0.71 J/cm^2 and a smaller vacuole at fluence 0.4 J/cm^2 (500×).

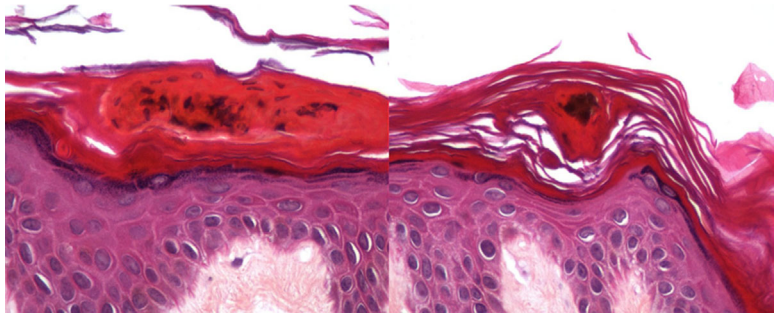

Fig. 7. These figures show the development and extrusion of a mends zone over time. In the left and right photos biopsy was taken 5 days and 2 weeks post treatment, respectively (400×).

intra-epidermal injury in the stratum spinosum characterized by vacuoles at the site of the high fluence zones. As measured with confocal microscopy and H&E staining, the stratum corneum and all tissue surrounding the vacuoles appeared normal with no indication of collateral thermal damage. This injury profile is in stark contrast to epidermal and dermal damage apparent in non-ablative and ablative fractional treatments. In a recent clinical study with a fractional picosecond Alexandrite laser, these localized epidermal vacuoles were associated with the deposition of new dermal collagen, elastic tissue, and mucin [4]. Keratinocytes produce a number of growth factors, chemokines, and cytokines in response to injury or a wound [8]. These factors and agents could stimulate and regulate the response to this injury through receptors on epidermal and dermal cells. It has been speculated that the rapid vacuole formation with the generation of an LIOB could create a pressure fluctuation in the skin [9]. This could also result in the initiation of dermal remodeling from changes in cell signaling and the release of cytokines from alterations in cellular membranes [6,10].

The high fluence zones created vacuoles, but the likelihood of this depended on the fluence within the zones, that is, the diffractive lens array and the amount of pigmentation. In darker skin types with high melanin content the confocal microscopic signatures were distinctly bright, quasi-spherical regions presumably due to light scattered from cellular debris consisting of nuclei and

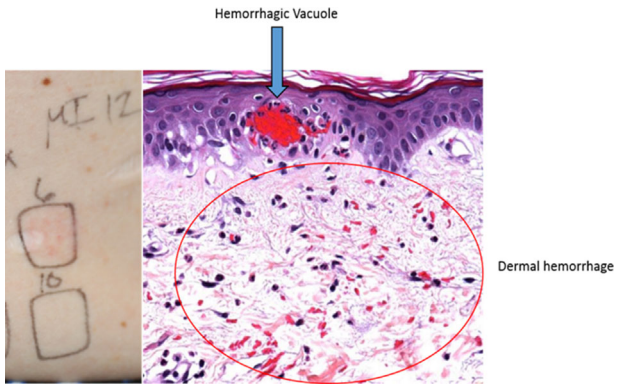

Fig. 8. Subject with skin type II, MI 12 treated in non sun-exposed area demonstrating pin point hemorrhage at 24 hours post. Histology reveals vacuoles at the dermal epidermal junction filled with blood and adjacent dermal hemorrhage (200×).

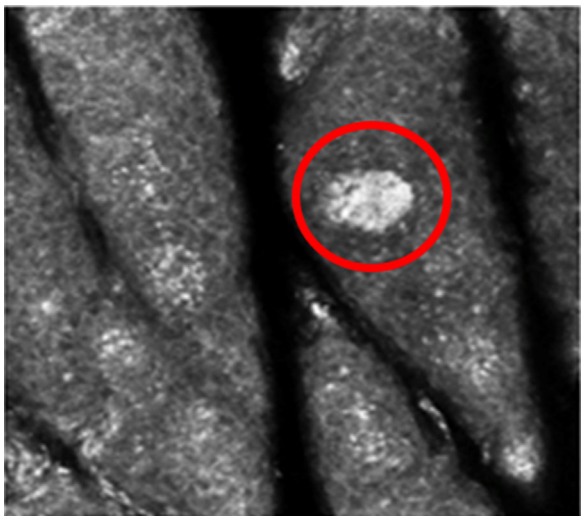

Fig. 9. Confocal microscopy image 24 hours post treatment of the volar forearm with MI = 32 at $F = 0.71\,\mathrm{J/cm^2}$. Bright vacuole in circle.

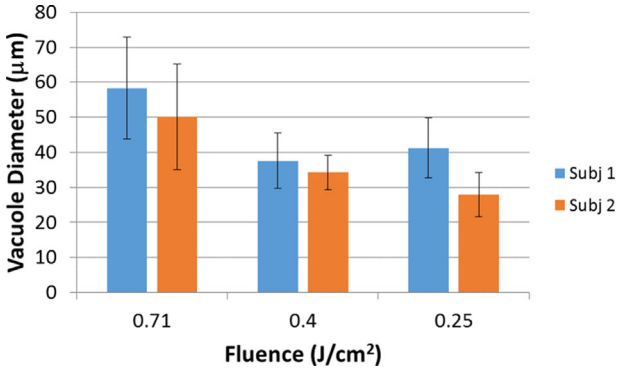

Fig. 10. Vacuole diameters measured with confocal microscopy (skin type IV, MI = 31, 32).

melanosome clusters within the vacuoles. As the melanin content of the epidermis decreased, the size, location, and prevalence of the vacuoles also decreased. In lighter skin types the injury profile dramatically changed. In histology the vacuoles accompanied by hemorrhage were found at the dermal-epidermal junction. The vascular injury was only seen at the higher fluence $F = 0.71\,\mathrm{J/cm^2}$. The extent of vascular involvement depended on MI, decreasing with increasing skin melanin concentration. The target chromophore apparently had shifted to include hemoglobin in the superficial capillary loops. These findings illustrate the importance of melanin in confining the injury to vacuoles in the epidermis and suggest a fluence threshold for vacuole formation dependent on skin pigment concentration.

The role the vacuoles play in bringing about clinical outcomes is a subject of further investigation but the physical process leading to their formation is known to proceed by a complex sequence of steps. The creation of vacuoles in retina by laser heating has been reported and analyzed theoretically in the literature [11]. The theory posited expansion of a steam bubble created by laser heating of retinal melanin. A short laser pulse (less than microseconds) resulted in essentially instantaneous heating followed by expansion of the bubble long after the pulse had ended. In the present case, the target chromophore is the melanin in the epidermis. However, absorption of laser radiation by these granules alone is insufficient explain the observed bubble formation. A chromophore with 100 times greater absorbance is required. Such a highly absorbing chromophore can be created transiently by the laser radiation, in a process known as Laser Induced Optical Breakdown (LIOB). In the LIOB process thermionic emission of one or more electrons from laser-heated melanin provides initial free "seed" electrons during the laser pulse

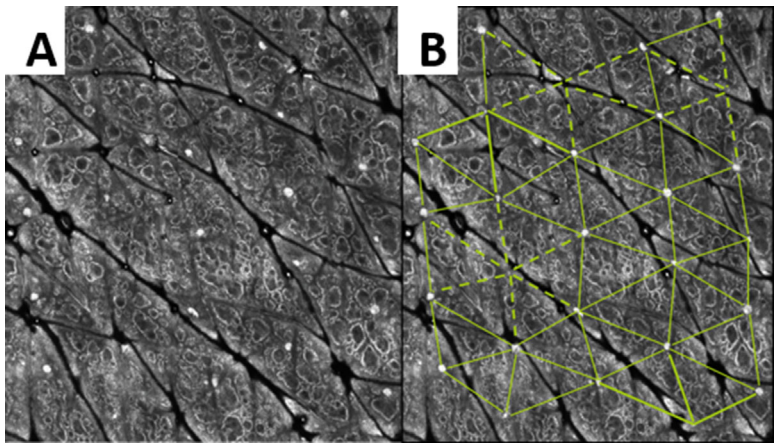

Fig. 11. (**A**) Approximately 40 μm below the skin surface small vacuoles are seen in the epidermis corresponding to the vacuoles noted on microscopic examination. (**B**) Connecting these spaces reveals a grid pattern of the fractional optic with similar pitch.

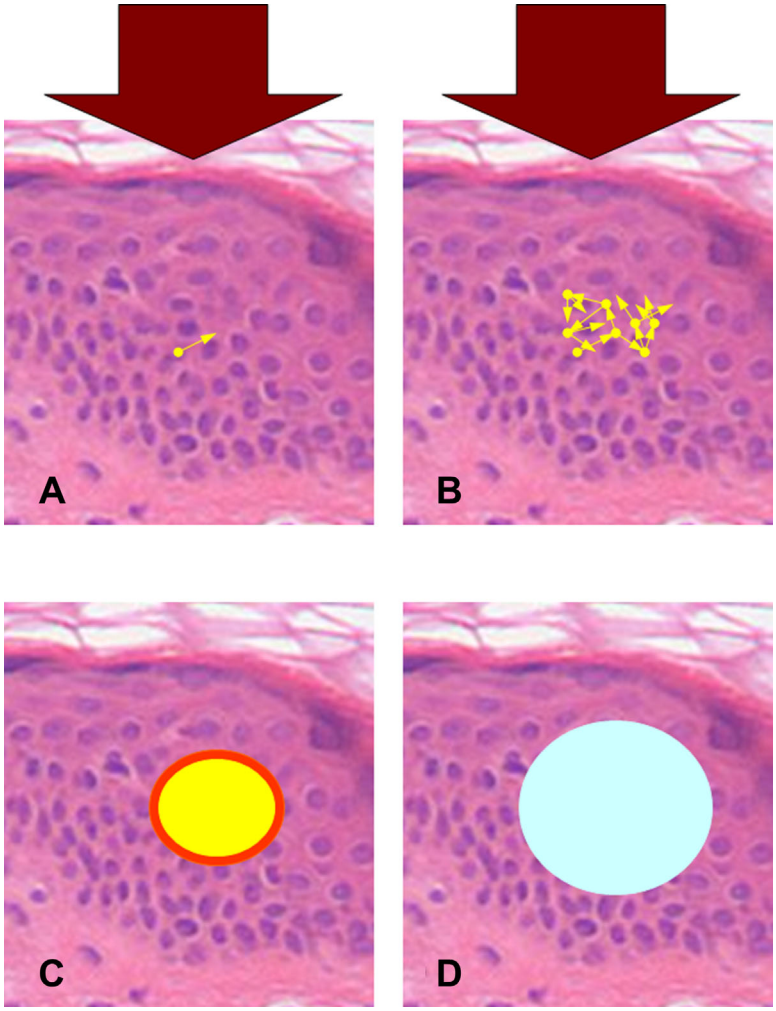

Fig. 12. Process of vacuole formation in the epidermis: (**A**) A high intensity portion of the laser beam created by the diffractive lens array irradiates a region of the skin. A seed electron is ejected from an absorber (melanin) (**B**) The number of free electrons grows in an avalanche process. Electron plasma density increases absorbing energy from the beam (**C**) The laser beam terminates leaving a hot plasma ball. The plasma ball rapidly heats the surrounding tissue above boiling temperature (**D**) Steam expansion creates a vacuole in the epidermis.

(Fig. 12A). Free electrons very efficiently absorb the laser light to gain energy between collisions with the surrounding molecules. When the energy of the seed electron exceeds that required to ionize a melanin molecule the next collision can result in the generation of a second free electron. This process repeats and the free electron density and energy grow to form an ionized plasma that continues to absorb very efficiently the remaining laser radiation of the pulse. The resulting hot plasma heats the surrounding tissue via electron-molecule collisions even after the laser pulse has ended (Fig. 12C). Theoretical analysis shows that the energy of the plasma is sufficient to create a steam bubble causing the intra-epidermal vacuoles (Fig. 12D) [12].

The process for LIOB formation relies on the generation of initial seed electrons to efficiently absorb the laser radiation. The generation of these electrons by means of thermionic emission is statistical in nature. Theoretical analysis to be presented elsewhere relates the probability of thermionic emission to the laser parameters and melanin concentration. The greater the laser fluence or melanin concentration, the earlier in the laser pulse a seed electron will initiate LIOB formation. This means more energy in the remaining pulse is absorbed by the electron plasma to create larger vacuoles. In light-skinned subjects the probability of LIOB formation is greatest in the deeper region of the epidermis, in proportion to the epidermal melanin concentration [7]. Hemorrhagic vacuoles within the epidermis or superficial papillary dermis suggest that the LIOB process itself can either disrupt neighboring blood vessels or be initiated by hemoglobin [13].

A limitation of this study was that the number of subjects was insufficient to obtain statistical significance in the analysis of vacuole size and depth versus fluence and melanin concentration. These results only suggest trends

or tendencies that support a theoretical analysis to be presented elsewhere.

CONCLUSIONS

A new type of epidermal injury created by a picosecond Alexandrite laser with a fractional lens array has been described. The results suggest that melanin is the primary target capable of generating laser induced optical breakdown leading to focal vacuoles in the epidermis. This closed injury is associated with the production of dermal collagen, elastic tissue, and mucin with minimal post treatment downtime.

ACKNOWLEDGMENT

This study was supported by research funding from Cynosure, Inc. in 2013.

REFERENCES

1. Manstein A, Herron GS, Sink RK, Tanner H, Anderson RR. Fractional photothermolysis: A new concept for cutaneous remodeling using microscopic patterns of thermal injury. Lasers Surg Med 2004;34(5):426–438.
2. Lloyd J, Tanghetti E. Comparison of affirm 1320/1440 nm vs 1320 nm for the treatment of acne scars—A clinical and histological study. Lasers Surg Med 2008;40(S20):66.
3. Tanghetti E, Weiss R. Multicenter study of microthermal laser treatment of acne scars. Lasers Surg Med 2007;39(S19): 112.
4. Brauer JA, Kazlouskaya V, Alabdulrazzaq H, Bae YS, Bernstein LJ, Anolik R, Heller PA, Geronemus RG. Use of a picosecond pulse duration laser with specialized optic for treatment of facial acne scarring. JAMA Dermatol 2015;151(3):278.
5. Tanghetti E, Tanghetti M. A clinical and histologic study of skin treated with a pico-second alexandrite laser comparing a uniform treatment spot and a spatially modulated spot. Lasers Surg Med 2014;46(S25):86.
6. Tanghetti E. Characterization of the histologic changes in the skin from the treatment with the 755 nm Picosecond Alexandrite Laser. Lasers Surg Med 2015;47(S26):24.
7. Nielsen KP, Zhao L, Ryzhikov GA, Biryulina MA, Sommersten ER, Stamnes JJ, Stamnes K, Moan J. Retrieval of the physiological state of the human skin from UV-Vis reflectance spectra—A feasibility study. J Photochem Photobiol B 2008;93:23–31.
8. Werner S, Krieg T, Smola H. Keratinocyte-fibroblast interactions in wound healing. J Invest Dermatol 2007; 127(5):998–1008.
9. Vogel A, Busch A, Parlitz U. Shock wave emission and cavitation bubble generation by picosecond and nanosecond optical breakdown in water. J Acoust Soc Am 1996;100(1):148.
10. McDaniel D. Gene expression analysis in cultured human skin fibroblasts following exposure to a picosecond pulsed alexandrite laser and specially designed focus optic. Lasers Surg Med 2015;47(S26):22.
11. Gerstman BS, Thompson CR, Jacques SL, Rogers ME. Laser induced bubble formation in the retina. Lasers Surg Med 1996;18(1):10–21.
12. Mirkov M, Sierra R, Tanghetti E. Theoretical analysis of the mechanism producing the histologically observed epidermal changes with a picosecond alexandrite laser with Diffractive Lens Array. Lasers Surg Med 2016;48(S27):1.
13. Habbema L, Verhagen R, Van Hal R, Liu Y, Varghese B. Minimally invasive non-thermal laser technology using laser-induced optical breakdown for skin rejuvenation. J Biophotonics 2012;5(2):194–199.